CRYSTAL GROWTH & DESIGN
2008
VOL. 8, NO. 5
1675–1681

Explanation for the Emergence of a Single Chiral Solid State during Attrition-Enhanced Ostwald Ripening: Survival of the Fittest

Wim L. Noorduin,[†] Hugo Meekes,*[,†] Arno A. C. Bode,[†] Willem J. P. van Enckevort,[†] Bernard Kaptein,[‡] Richard M. Kellogg,[§] and Elias Vlieg[†]

IMM Solid State Chemistry, Radboud University Nijmegen, Toernooiveld 1, 6525 ED, Nijmegen, The Netherlands, DSM Pharmaceutical Products−Advanced Synthesis, Catalysis & Development, P.O. Box 18, 6160 MD, Geleen, The Netherlands, and Syncom B.V., Kadijk 3, 9747 AT, Groningen, The Netherlands

Received December 10, 2007; Revised Manuscript Received January 30, 2008

ABSTRACT: The overabundant occurrence of single-handed chiral molecules in living systems has inspired scientists for well more than a century. A route to the evolution of a single chiral solid phase, using abrasive grinding of the crystals in contact with a saturated solution, has been demonstrated for the achiral compound $NaClO_3$[1] crystallizing in a chiral space group and, recently, for an intrinsically chiral amino acid derivative.[2] In order to obtain insight in the complex processes involved in these experiments, we developed a computer model that is based only on attrition and Ostwald ripening. We find that, besides the relative rates of attrition and Ostwald ripening, the racemization efficiency in the solution is an essential parameter in the deracemization process. For high efficiency the evolution to single chirality is stochastic, whereas for lower values the process becomes increasingly deterministic and the handedness of the single chiral solid end state is readily controllable. The results show excellent agreement with experimental data and allow a further optimization of this promising deracemization technique.

Introduction

The single handedness of chiral molecules like sugars and amino acids, as evolved from a (presumably) racemic prebiotic world, has intrigued scientists ever since Louis Pasteur separated enantiomorphic sodium ammonium tartrate crystals.[3] Several mechanisms that lead to an imbalance between enantiomers have been proposed together with an amplification mechanism as an explanation for the origin of biomolecular single handedness. One class consists of autocatalytic reactions in which a small initial asymmetry is amplified, as was outlined by Frank and by Calvin and experimentally confirmed by Soai in a solution phase reaction.[4–7] Crystallization is an alternative route to chiral purification if the system behaves as a conglomerate.[8] This has been explored for racemizing systems under far from equilibrium conditions, for which the hard to control process of primary nucleation dictates the resolution outcome.[9–19]

In an intriguing experiment, Viedma demonstrated for $NaClO_3$,[1] which is intrinsically achiral but crystallizes in the chiral space group $P2_13$, that starting from a mixture of enantiomorphic crystals in contact with an achiral saturated solution, abrasive grinding can lead to a solid state of single chirality. This near-equilibrium technique is applicable not only to conglomerate forming salts but also to racemic conglomerates of intrinsically chiral compounds that racemize in solution.[20,21] Experimental demonstration of the latter process was recently reported for an amino acid derivative (**1**) (Scheme 1).[2] In both the experiments with $NaClO_3$ and the amino acid derivative **1**, small enantioimbalances in the solid phase inexorably result in a complete solution-mediated conversion of the minor chirality into the originally more abundant crystal phase.

In this study we give insight into the underlying principle of this complete symmetry breaking. So far, computational models designed to explain Viedma's results rely on the presence of primary nucleation,[22,23] but this is both unlikely and not necessary, as we will show. As a starting point we use Viedma's suggestion that this process is driven by the counteracting combination of Ostwald ripening and attrition.[24] Such a process implies near-equilibrium conditions, a situation in which primary nucleation is unlikely to occur. Using computational modeling we show that the combined processes of attrition and Ostwald ripening indeed result in the evolution of a single chiral solid phase. The model leads to both the breaking of the initial symmetry and the further enantiomeric enrichment, which is maintained once a solid phase of single chirality is reached. We derive a simple first-order kinetics description of the process, which is in excellent agreement with experimental observations[2] and provides further insight for process optimization. The results are quite insensitive to the details of the model and its parameters, suggesting that attrition-enhanced Ostwald ripening offers a robust pathway to single chirality.

Scheme 1. Evolution of a Single Chiral Solid Phase during the Process of Abrasive Grinding for *N*-(2-Methylbenzylidene)phenylglycine Amide 1 (compound 1 racemizes in solution in the presence of 5 mol % of DBU)

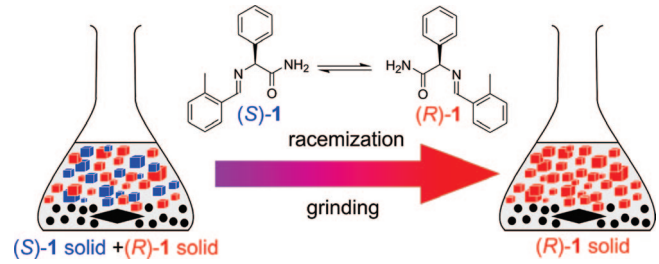

Ostwald Ripening. According to the Gibbs–Thomson effect, small particles have a higher solubility than large ones.[25] This is a direct consequence of the surface to volume ratio of the particles as the system minimizes its total surface free energy. In a saturated solution in contact with crystals, this leads to a process called Ostwald ripening: large crystals grow at the cost of smaller ones.[26] The thermodynamic ground state is therefore

* To whom correspondence should be addressed. E-mail: Hugo.Meekes@science.ru.nl.
[†] Radboud University Nijmegen.
[‡] DSM Pharmaceutical Products.
[§] Syncom B.V.

10.1021/cg701211a CCC: $40.75
Published on Web 04/16/2008

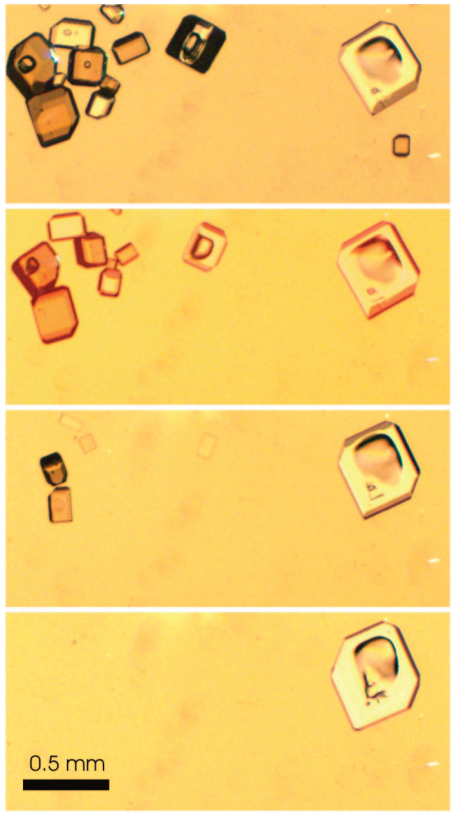

Figure 1. Polarized light microscope images showing the process of Ostwald ripening of $NaClO_3$ leading to a single chiral solid phase. A racemic mixture of $NaClO_3$ crystals in equilibrium with a saturated solution was studied. Under temperature-controlled conditions no significant deracemization was observed in two months. Under conditions with temperature fluctuations of ±2 °C, the process of crystallization and dissolution is enhanced, leading to one single crystal in two months in the observed region. The chirality of the crystals can be determined by rotating one of the crossed polarizers slightly either clockwise or counterclockwise. As a result, the L or D crystals, respectively, become dark.

one single crystal. As shown in Figure 1, this has an interesting consequence for a system of chiral crystals in contact with an achiral or racemizing solution: the thermodynamic stable state is one single, and therefore enantiopure, crystal. In other words, Ostwald ripening always leads to complete chiral deracemization in these systems. Reaching a single crystal end state for macroscopic crystals through Ostwald ripening takes a long time, typically months or even longer, depending on the system volume, the solubility, the rate of racemization in the solution, and the surface free energy.[27] For an initial crystal size distribution (CSD) with a large number of small crystals Ostwald ripening is fast, but its rate decreases rapidly as the CSD evolves toward large crystals. Because the final CSD is of no importance for the chiral purity, the advantage of small crystals speeding up the Ostwald ripening can be exploited in the deracemization process. A way to arrive at a CSD with many small crystals is to induce attrition by stirring or milling. This attrition also creates rough surfaces and stress, which further enhances the ripening process.

Computational Method

In order to better understand how the interplay between Ostwald ripening, leading to larger crystals, and attrition, leading to smaller crystals, can yield a single chiral state with many small crystals, a computer model containing the essential features of these two processes

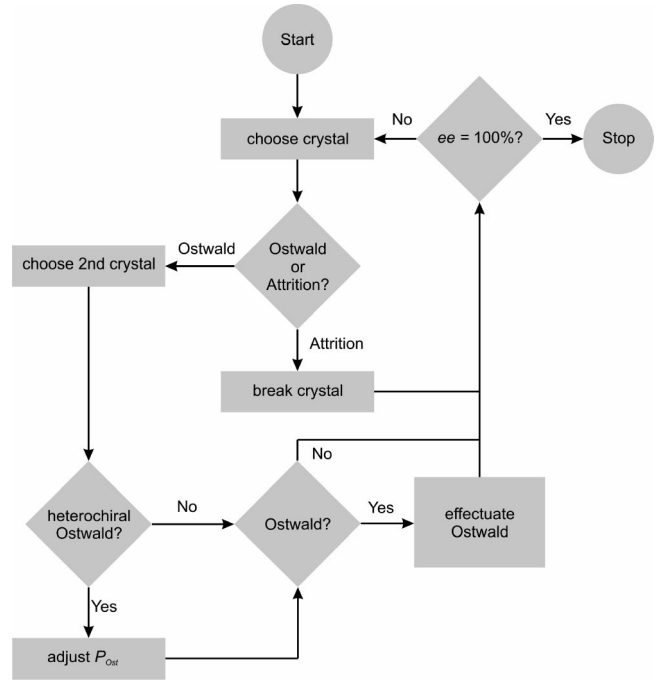

Figure 2. Flow diagram of the Monte Carlo simulation modeling the combined processes of Ostwald ripening and attrition.

was developed. A system consisting of a saturated solution, a reservoir with a constant number of achiral or racemizing molecules, in contact with the two CSDs of the enantiomers was subjected to a Monte Carlo simulation. The Monte Carlo process involves changes in the CSDs. The system has a constant total number, N, of molecules. With every Monte Carlo move, which mimicks a given time interval in a real experiment, for a randomly chosen crystal either attrition or Ostwald ripening occurs (Figure 2). The attrition−ripening ratio, ξ, is parametrized as the ratio between the probability of an attrition event, P_{attr}, and the probability of an Ostwald event, P_{Ost},

$$\xi = \frac{P_{attr}}{P_{Ost}} \tag{1}$$

The attrition−ripening ratio, to be interpreted as a measure for the stirring intensity, can also be regarded as a reciprocal measure for the exchange rate of solute, which, among others, is determined by the solubility. The higher this rate, the more effective the Ostwald ripening, and the smaller the attrition−ripening ratio. In an attrition event the crystal is broken into two pieces of arbitrary size. The only restriction is that the total number of molecules remains constant. Because in practice grinding is effective down to a minimal crystal size, attrition is only allowed above a minimal size in terms of the number of molecules n_{min}. Throughout this paper n_{min} is set to 10. For an Ostwald ripening event a second crystal is randomly selected. The largest of the two crystals may gain a single molecule at the cost of the other crystal. The probability that this event occurs for a crystal with n_i molecules to a crystal with n_j molecules (Supporting Information) is

$$P_{Ost}(n_i, n_j) = P_{Ost}\left(\frac{1}{\sqrt[3]{n_i}} - \frac{1}{\sqrt[3]{n_j}}\right) \tag{2}$$

In this equation linear growth/dissolution kinetics are assumed as the crystal surfaces are roughened by the grinding process. In a Monte Carlo process the events occur consecutively, whereas in a real experiment events take place simultaneously. The simulation time is therefore scaled with the number of crystals present in the CSD on each event.

The chiral identity of $NaClO_3$ molecules is instantaneously lost upon dissolution. In the experiment in which chiral molecules racemize in solution, the situation is more complex, as the time scales of racemization and Ostwald ripening differ. The exchange rate of

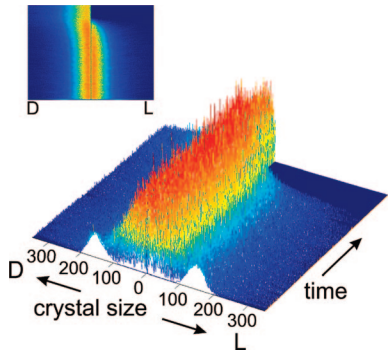

Figure 3. Typical example of the crystal size distribution of D and L crystals during a Monte Carlo run simulating the combined process of attrition and Ostwald ripening for a compound racemizing in solution. The initial CSD is set to a racemic mixture of two Gaussian distributions each containing 10^5 molecules centered around a crystal size of 150 molecules. The attrition−ripening ratio is set to $\xi = 0.01$; and the racemization efficiency to $\chi = 0.1$. The graph shows the evolution of the CSD during 1.8×10^8 Monte Carlo events. The inset shows a top view of the graph.

molecules between the solution and the crystals is high compared to the process of racemization in solution. We therefore need to distinguish between a homochiral and a heterochiral event for Ostwald ripening. For a heterochiral event a molecule will attach to a crystal of the opposite handedness, only after having attained the correct handedness as a result of racemization. The probability for "heterochiral Ostwald ripening" is therefore reduced compared to a homochiral event, for which a dissolved molecule preserves its chirality and attaches to a crystal of the same handedness. To take account of this difference in the model, we reduce the chance for Ostwald ripening if the chosen crystal pair is of opposite chirality, using a racemization efficiency parameter χ according to

$$P_{\mathrm{Ost}} = \begin{cases} P_{\mathrm{Ost}} & \text{(homochiral)} \\ \chi P_{\mathrm{Ost}} & \text{(heterochiral)} \end{cases} \tag{3}$$

For a system in which the racemization is instantaneous $\chi = 1$, whereas in the absence of solution racemization $\chi = 0$.

The enantiomeric excess (ee) of the solid phase during a simulation run is computed from $\mathrm{ee} = (N_{\mathrm{D}} - N_{\mathrm{L}})/(N_{\mathrm{D}} + N_{\mathrm{L}})$, where N_{D} and N_{L} are the number of D and L molecules, respectively, in the solid phase. Note that primary nucleation is not included in the model, as the actual solution is nearly saturated during the whole process. Even if the formation of primary nuclei would be included and a nucleus with the minority chirality should form, it would rapidly dissolve because of its large undersaturation with respect to the larger crystals.

Results and Discussion

Initial Racemic Conglomerate. Figure 3 presents the typical development of the CSDs of the two opposite chiral solids during a Monte Carlo run for $\xi = 0.01$ and $\chi = 0.1$. The simulations start with equal Gaussian-shaped CSDs, although the exact shape is not important, as the initial CSDs are rapidly broadened around small average crystal sizes. The system *always* evolves into a single chiral end state. Once the last minority enantiomer crystal is dissolved, the single chiral solid phase remains in a steady state consisting of many small crystals of one enantiomer as long as the attrition is sustained. When the attrition is stopped (no stirring), the single chiral state persists, as primary nucleation is not allowed, and Ostwald ripening will lead to a CSD with increasingly large crystals (not shown in Figure 3). By performing many such simulations we find that the final single chiral end state is randomly D or L for these conditions.

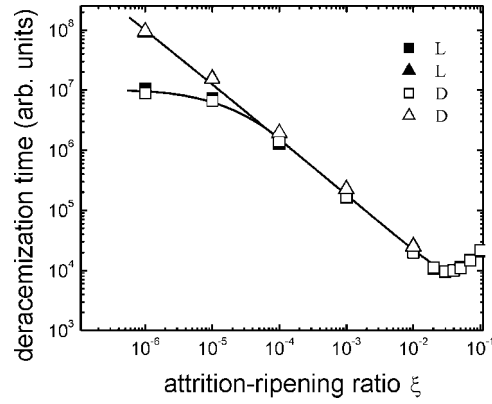

Figure 4. Average deracemization time t_{derac} as a function of the attrition−ripening ratio ξ for a compound racemizing in solution ($\chi = 0.1$), with either D (open symbols) or L (full symbols) final state. The initial ee = 0. Results are averages of 100 simulation runs and are shown for two system sizes: $N = 2 \times 10^4$ (square symbols), $N = 2 \times 10^5$ (triangle symbols). The line is drawn as a guide to the eye.

The time to reach a single chiral end state depends on the simulation parameters. Figure 4 presents the deracemization time t_{derac}, as a function of the attrition−ripening ratio ξ for $\chi = 0.1$. As expected, the deracemization times for either the L or the D state are equal. For small attrition−ripening ratios, t_{derac} is large, as the system consists of only a few large crystals, a situation that is similar to Figure 1. This leads to long deracemization times. For intermediate values of the attrition−ripening ratio the crystals stay sufficiently small for the Ostwald process to be effective, resulting in a reduction of t_{derac} by several orders of magnitude. When applying very intense stirring, the CSDs narrow as they move to many crystals with sizes close to the minimal size for attrition, n_{min}, and Ostwald ripening becomes less effective as the differences in driving force become small and the attrition destroys large crystals. Figure 4 also shows that the deracemization time is independent of the size N of the system for intermediate and high values of the attrition−ripening ratio. This is in good agreement with experimental results for an amino acid derivative.[2] In the case of instantaneous racemization in solution ($\chi = 1$), the deracemization process evolves in a comparable fashion (Supporting Information Figures SI 1 and 2). There is, however, one essential difference. For $\chi = 1$ the system behaves more stochastically and the deracemization time scales linearly with the system size (Figure SI 3).

Initial Enantiomeric Excess. In the discussion so far, we have started with equal initial CSDs and therefore an ee of zero. To compare the model with the experimental results obtained with an initial enantioimbalance,[1,2] we simulated the effect of an excess amount in one enantiomer, while at the same time keeping the initial mean crystal sizes and variances equal for both distributions. For a racemization efficiency of $\chi = 0.1$ and various initial values of the enantiomeric excess we determined the ee for 1600 simulation runs as a function of time. An initial enantiomeric excess of merely 2.5% caused *all* runs to evolve irreversibly and completely toward this enantiomer in excess. In Figure 5, the ee as a function of time is presented for nine individual simulation runs with different starting ee's. As the figure shows, even small imbalances in the initial ee are effectively amplified to an enantiomeric pure end state, which is in good agreement with the experimentally observed results.[1,2] However, performing these simulation runs for instantaneous racemization in solution, i.e., $\chi = 1$, we find no chiral amplification but only stochastic behavior toward a single chiral end state (see Figure SI 4). This seems to be in contradiction with

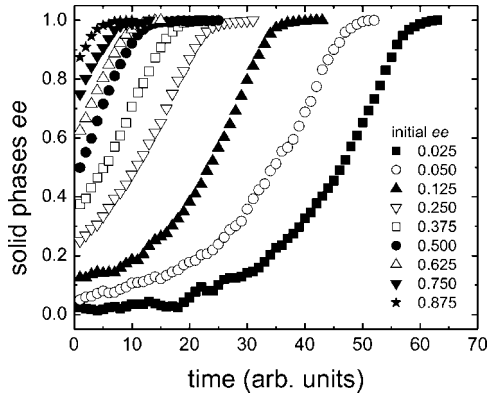

Figure 5. Enantiomeric excess versus time for the racemizing system ($\chi = 0.1$) for small imbalances in the initial ee. $N = 8000$; $\xi = 0.04$.

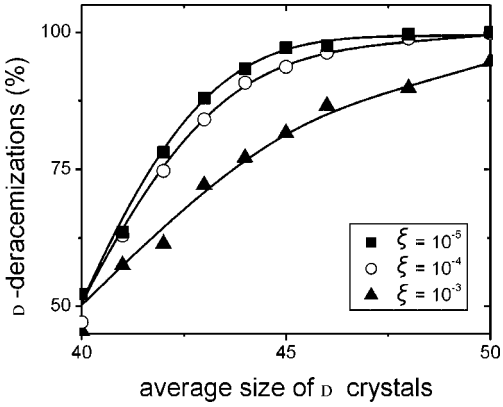

Figure 6. Influence of shifted CSDs on the deracemization outcome for an intrinsically racemic solution ($\chi = 1$). Shown is the percentage of runs ending in pure D averaged over 1000 simulations as a function of the shift of the initial CSDs of the D enantiomer while keeping the ee equal to zero for the two enantiomers. The initial CSD of the L crystals was kept constant around 40 molecules. The curves represent various attrition−ripening ratios ξ. $N = 10^4$. The lines are a guide to the eye.

the amplification observed in $NaClO_3$,[1] which promptly loses its chiral identity upon dissolution. Therefore, we studied another form of initial asymmetry, namely, that caused by a relative shift of the CSD of one of the enantiomers.

Shifted CSDs. The size of the crystals plays an important role. In practice, the initial CSDs of both enantiomers of the conglomerate will never be completely equal, in contrast to our simulations so far. Therefore, we modeled the deracemization process for $\chi = 1$ with slightly shifted starting CSDs, while keeping the initial ee zero. The results are shown in Figure 6. Shifting one of the CSDs results in a higher probability of reaching the end state corresponding to the initially larger crystals. This amplification is strongest at low values of the attrition−ripening ratio. For these low values of ξ, the CSD "memory" will exist long enough to induce a sufficient increase in overall ee and to direct the system toward the correct single chiral state, whereas this memory is rapidly lost if very small crystals are formed by strong attrition. In the latter case, the outcome of the deracemization is more stochastic.

These results might explain the earlier mentioned experiments performed by Viedma,[1] in which he studied the effect of an initial excess in one of the enantiomers. Small imbalances in the initial CSD may have been amplified effectively to a

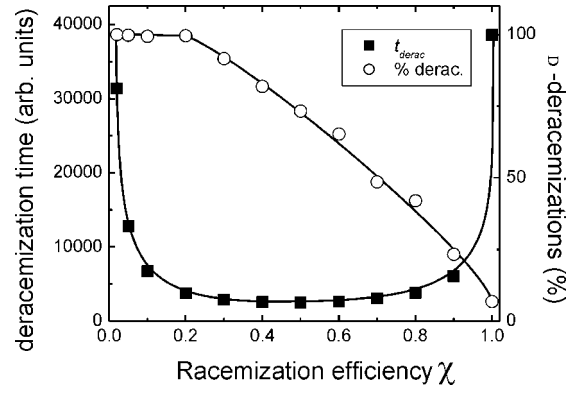

Figure 7. Deracemization time as well as the percentage of the deracemizations ending in pure D averaged over 1600 simulations as a function of the racemization efficiency χ for $\xi = 0.04$ and an initial ee = 5% in D. Lines are a guide to the eye.

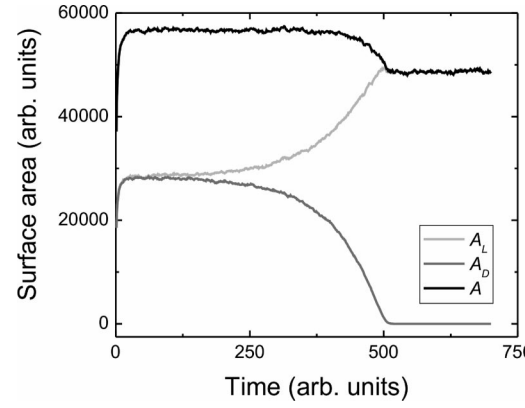

Figure 8. Total crystal surface area during the deracemization process shown in Figure 3 with A_D and A_L being the total crystal surface areas of the D and L crystals, respectively, and A the sum of these two.

deterministic end state of single chirality of the handedness of the initially larger crystals. Another mechanism that may play a role in the case of $NaClO_3$ is that in addition to single molecules also small clusters that are still chiral are exchanged in the Ostwald process. For such clusters heterochiral events are not possible. This corresponds to a situation for which $\chi < 1$, i.e., a situation for which an initial enantiomeric excess will be amplified.

Racemization Efficiency χ. In order to understand the influence of the racemization efficiency on the enantiomeric enrichment, Figure 7 presents the deracemization time versus the racemization efficiency χ for $\xi = 0.04$, starting with ee = 5%. The bathtub-shaped graph shows that a minimal deracemization time is accessible for a wide range of χ values. The graph also shows the chance that the system evolves to the enantiomer initially in excess. For $\chi < 0.2$ this chance is virtually 100%, and it decreases almost linearly for higher values of χ up to the level that stochasticity completely dominates the deracemization outcome for $\chi = 1$.

Time Dependence of the Deracemization Process. The deracemization described here is a near-equilibrium process in which the combined processes of dissolution and crystallization in the absence of attrition would result in a slowing down of enantiomeric purification as a result of the CSDs evolving to larger crystals. The crystals are, however, continuously broken by grinding, which leads to quasi steady state CSDs, as can be seen in Figure 3. The CSDs change appreciably only at the very

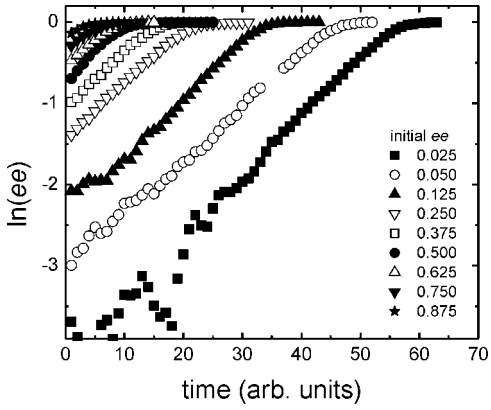

Figure 9. ln(ee) versus time for the experiments with small initial imbalances in the ee (Figure 5).

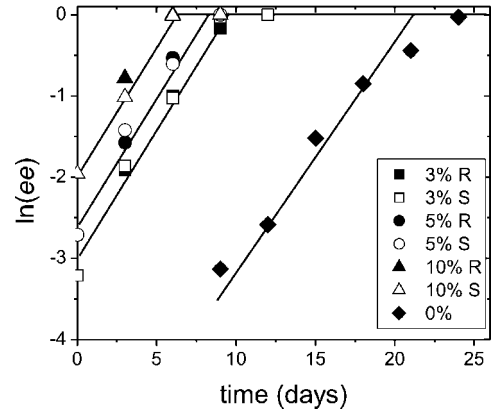

Figure 10. Logarithm of the ee versus time for various initial ee's of an amino acid derivative in acetonitrile. The data are obtained from Figure 1 in ref 2. All ee values have been determined using chiral HPLC, except for the values at $t = 0$, which were calculated from the initial solid ee values and corrected for the solubility. The HPLC detection limit is estimated to be ee $\approx$ 5%. The lines are drawn as a guide to the eye.

beginning of the deracemization process and at the end, where the ee approaches unity. Figure 8 shows that the corresponding total crystal surface area, A, remains approximately constant during the major part of the process. Therefore, we can write

$$A_D(t) + A_L(t) \approx A \tag{4}$$

with A_D and A_L being the total crystal surface areas of the solids of D and L, respectively. We observe that a small initial ee of one enantiomer results in the emergence of a single chiral solid phase of the initially most abundant enantiomer. This deracemization is driven by the process of Ostwald ripening. During the major part of the deracemization, the Ostwald process leads to a transfer of crystal surface area from one enantiomer to the other, as can be seen in Figure 8. Overall, the number of successful Ostwald events per time interval, corresponding to the attachment of a molecule to the crystal surface of the increasing population and the detachment of a molecule from the surface of the decreasing population, is linearly dependent on the difference in available crystal surface area of the two populations. Therefore, one can write the conversion of the solids in time as

$$-\frac{dA_L}{dt} = \frac{dA_D}{dt} = k(A_D - A_L) = k(2A_D - A) \tag{5}$$

with k being the rate constant for a given attrition−ripening ratio. After integration this results in

$$\ln\left[\frac{2A_D(t) - A}{2A_D(0) - A}\right] = kt \tag{6}$$

for solid D. This equation can be expressed as a function of the enantiomeric excess in the solid phase assuming steady state normalized CSDs for both populations:

$$ee = \frac{N_D - N_L}{N_D + N_L} \approx \frac{A_D - A_L}{A_D + A_L} = \frac{2A_D - A}{A} \tag{7}$$

resulting in

$$ee(t) = ee(0)\exp(kt) \tag{8}$$

The initial ee is thus amplified exponentially. This first-order kinetics expression can now be used to fit the simulated as well as the experimental results. Figure 9 shows a plot of ln(ee) versus time for the deracemizations of Figure 5. Clearly an exponential behavior is observed for the major part of the deracemization process. The experimental results[2] for compound **1** are plotted in Figure 10 for various values of the initial ee. In both figures the deracemization rate constant k turns out to have approximately the same value for all initial enantioimbalances. The rate constant k does depend, however, on the attrition−ripening ratio ξ (Figure 4) and the racemization efficiency χ (Figure 7). This was recently confirmed experimentally by the observation that adding more base, which catalyzes racemization, to the system of compound **1** shortens the deracemization times considerably.[28]

Mechanism. In the deracemization process an imbalance in the populations of the two enantiomers, caused either by an initial enantioimbalance or stochastically by attrition, leads to a single chiral end state. Two mechanisms play a crucial role. The stochastic process of attrition leads to a nondeterministic evolution of the system. On the other hand, if the racemization mechanism is not instantaneous, the homochiral Ostwald ripening is more effective than the heterochiral. This drives the system deterministically to an end state corresponding to the larger crystals (Figure 3 and SI 1). To understand the interplay of the two mechanisms, we consider a system with initially isomorphous CSDs for various values of χ and ξ (Figure 11).

- We first consider the case for which $\chi = 0$ and $\xi = 0$, that is, a stagnant solution in which no racemization is involved. In that case, Ostwald ripening eventually leads to two single crystals of either handedness. This process will be very slow. An initial imbalance in the population of the solids of the two enantiomers, with isomorphous CDSs, leads to the lowest Gibbs free energy for the enantiomer in excess as a result of smaller surface to volume ratio.
- In the case $0 < \chi \ll 1$ and $\xi = 0$, that is, a stagnant solution in which the racemization rate is small compared to the rate of Ostwald ripening, the end state will eventually be a single crystal. The handedness of this crystal is still determined by the enantiomer initially in excess as a result of the slow racemization. Achieving the end state will take a very long time.
- If in addition attrition is applied ($\xi > 0$), the racemization rate will hardly be affected, but the rate of Ostwald ripening increases. The end state will therefore again be of single chirality consisting of many crystals of the enantiomer initially in excess

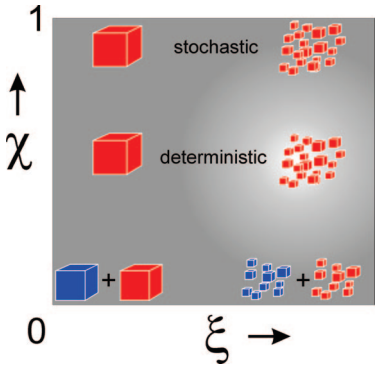

Figure 11. Schematic drawing of the end states of attrition-enhanced Ostwald ripening as a function of the racemization efficiency χ and the attrition−ripening ratio ξ starting from a racemic mixture of enantiomorphic crystals. For values of $\chi \approx 1$ the process is stochastic. For intermediate values of χ the end state is reached in a deterministic way, amplifying small initial imbalances. The background brightness is an indication of the minimal deracemization time.

(Figure 5). More importantly, the deracemization time will be smaller (Figure 4). The evolution to the end state will become less deterministic for values of the racemization efficiency approaching unity.

• In the limiting case of instantaneous racemization in solution ($\chi = 1$) the racemization rate and the Ostwald ripening rate are no longer distinguishable. As a result, the chance of finding either enantiomer as the end state equals the initial enantiomeric excess. This is clear for a stagnant solution ($\xi = 0$). In case of attrition, the model shows that this still holds (Figure SI 4).

In other words, the deracemization process is stochastic for instantaneous racemization in solution ($\chi = 1$). In the case of a stagnant solution the end state will have a lower Gibbs free energy. When attrition is applied, the CSDs rapidly reach a steady state situation. In this steady state, the relatively slow process of deracemization leads to a single chiral end state, without a further change in Gibbs free energy. This can be seen in the total crystal surface area, which remains constant (Figure SI 2). Thus, there is no overall thermodynamic driving force in the case of instantaneous racemization, and the single chiral end state is a trap from which the system will not escape as long as there is no primary nucleation. The situation is different for noninstantaneous racemization in solution ($\chi < 1$). During the deracemization the increasing imbalance in the populations of the two enantiomers leads to an increasing frequency for the homochiral Ostwald ripening events for the enantiomer in excess. Therefore, the overall Ostwald ripening process becomes increasingly efficient for this enantiomer. The resulting decreasing total crystal surface area offers the overall driving force toward a lower Gibbs free energy, which can be seen in Figure 8.

Our explanation for the deracemization process is also relevant for a discussion in the recent literature on the driving mechanism behind the process.[20,21] Setting aside the dispute, which was a main item in that discussion, on how to interpret Gibbs' phase rule and Meyerhoffer's double solubility rule in such systems, we will address the most relevant points one-by-one.

(i) As we have shown, primary nucleation does not play an essential role in the process.

(ii) The arguments used in the discussion to determine the most stable state of the system overlook the fact that in a stagnant solution the only stable state is that of one single crystal, which obviously is enantiopure. Lowering the total surface free energy provides the driving force to that stable state.

(iii) A distinction between homochiral and heterochiral events is important in order to parametrize the racemization efficiency in the solution. Chiral clusters could play a role but are not needed to explain the deracemization process.

(iv) The distinction between noninstantaneously and instantaneously racemizing solutions is essential. It does not arise from Gibbs' phase rule, but from the effect it has on the way the system evolves to single chirality as described by the racemization efficiency parameter χ.

Conclusions and Implications

We have developed a model that explains the complex behavior of enantiomorphic crystals in contact with a solution in which racemization occurs, continuously perturbed by attrition. Simulations based on the model show that Ostwald ripening drives such a system to a single chiral end state for the solid phase. The deracemization time for the solid phase is determined by two parameters, namely, the attrition−ripening ratio ξ and the solution racemization efficiency χ. By choosing a moderate racemization efficiency, the handedness of the end state can be dictated by a small initial imbalance in the crystal size distributions (CSDs), either as an enantiomeric excess or as a relative shift in the size of the crystals. The evolution to the single chiral end state can, in that case, be described by first-order kinetics. The same behavior was found experimentally. The deracemization rate constant k can be increased by increasing the solution racemization efficiency χ. Paradoxically, the deracemization time for instantaneous racemization in solution ($\chi = 1$) is longer when compared with the case of relatively slow racemization ($\chi = 0.1$) (Figure 7). The reason for this is the stochastic behavior for $\chi = 1$, which is suppressed for smaller values of χ.

Thus, the model offers the ability to control and optimize this deracemization process under near equilibrium conditions.[28] The absence of the need for primary nucleation circumvents two drawbacks otherwise encountered.[29,30] The outcome of a process involving primary nucleation is difficult to control with a yield limited by the solubility of the compound. Therefore, the near-equilibrium deracemization process is a promising and robust tool of industrial importance for the production of enantiopure pharmaceuticals.

In a broader perspective, the combination of stochastic attrition and Ostwald ripening is a selection process based on the principle of survival of the fittest, the fittest group consisting of more and/or larger crystals. The results presented elucidate a suggested route to enantiopure molecules that form the building blocks for the evolution of life.

Note Added in Proof. During the printing of the manuscript the authors became aware of a publication by Cartwright et al., which discusses a model describing Viedma's experimental results, that is also based on Ostwald ripening, but including primary nucleation and without a racemization efficiency (Cartwright, J. H. E.; Piro, O.; Tuval, I. *Phys. Rev. Lett.* **2007**, *98*, 165501).

Acknowledgment. We would like to acknowledge Prof. D. G. Blackmond for stimulating discussions. The SNN agency (Cooperation Northern Netherlands) and the European Fund for Regional Development (EFRO) are acknowledged for partial support of this work.

Supporting Information Available: Derivation of formula 2; supplementary simulation results and results for the deracemization of **1**. This material is available free of charge via the Internet at http://pubs.acs.org.

References

(1) Viedma, C. *Phys. Rev. Lett.* **2005**, *94*, 065504.
(2) Noorduin, W. L.; Izumi, T.; Millemaggi, A.; Leeman, M.; Meekes, H.; van Enckevort, W. J. P.; Kellogg, R. M.; Kaptein, B.; Vlieg, E.; Blackmond, D. G. *J. Am. Chem. Soc.* **2008**, *130*, 1158.
(3) Pasteur, L. C. R. *Hebd. Séanc. Acad. Sci. Paris* **1848**, *26*, 535.
(4) Frank, F. C. *Biochim. Biophys. Acta* **1953**, *11*, 459.
(5) Calvin, M. *Molecular Evolution*; Oxford Univ. Press: Oxford, UK, 1969.
(6) Plasson, R.; Kondepudi, D. K.; Bersini, H.; Commeyras, A.; Asakura, K. *Chirality* **2007**, *19*, 589.
(7) Soai, K.; Shibata, T.; Morioka, H.; Choji, K. *Nature* **1995**, *387*, 767.
(8) Jacques, J.; Collet, A.; Wilen, S. H. *Enantiomers, Racemates and Resolution*; Krieger: Melbourne, FL, 1994.
(9) Havinga, E. *Chem. Weekblad* **1941**, *38*, 642.
(10) Havinga, E. *Biochem. Biophys. Acta* **1954**, *13*, 171.
(11) Barton, D. H. R.; Kirby, G. W. *J. Chem Soc.* **1962**, 806.
(12) Pincock, R. E.; Perkins, R. R.; Ma, A. S.; Wilson, K. R. *Science* **1971**, *174*, 1018.
(13) Addadi, L.; Berkovitch-Yellin, Z.; Domb, N.; Gati, E.; Lahav, M.; Leiserowitz, L. *Nature* **1982**, *296*, 21.
(14) Van Mil, J.; Addadi, L.; Lahav, M. *Tetrahedron* **1987**, *43*, 1281.
(15) Kondepudi, D. K.; Kaufman, R. J.; Singh, N. *Science* **1990**, *250*, 975.
(16) Kondepudi, D. K.; Bullock, K. L.; Digits, J. A.; Yarborough, P. D. *J. Am. Chem. Soc.* **1995**, *117*, 401.
(17) Cartwright, J. H. E.; García-Ruiz, J. M.; Piro, O.; Sainz-Díaz, C. I.; Tuval, I. *Phys. Rev. Lett.* **2004**, *93*, 035502.
(18) Plasson, R.; Kundepudi, D. K.; Asakura, K. *J. Phys. Chem. B* **2006**, *110*, 8481.
(19) Qian, R.-Y.; Botsaris, G. D. *Chem. Eng. Sci.* **1998**, *53*, 1745.
(20) (a) Crusats, J.; Veintemillas-Verdaguer, S.; Ribó, J. M. *Chem.−Eur. J.* **2006**, *12*, 7776. (b) Crusats, J.; Veintemillas-Verdaguer, S.; Ribó, J. M. *Chem.−Eur. J.* **2007**, *13*, 10303.
(21) (a) Blackmond, D. G. *Chem.−Eur. J.* **2007**, *13*, 3290. (b) Blackmond, D. G. *Chem.−Eur. J.* **2007**, *13*, 10306.
(22) Uwaha, M. *J. Phys. Soc. Jpn.* **2004**, *73*, 2601.
(23) Saito, Y.; Hyuga, H. *J. Phys. Soc. Jpn.* **2005**, *74*, 2.
(24) Viedma, C. *Astrobiology* **2007**, *7*, 312.
(25) Gibbs, J. W. *Thermodynamics, Collected works Vol. I*; Yale University Press: New Haven, CT, 1948.
(26) Ostwald, W. *Lehrbuch der Allgemeinen Chemie, Vol. 2, Part 1*; Leipzig, Germany, 1896.
(27) Beinfait, M.; Kern, R. *Bull. Soc. Fr. Mineral. Cryst.* **1964**, *87*, 604.
(28) Noorduin, W. L., et al. In preparation.
(29) Brands, K. M. J.; Davies, A. J. *Chem. Rev.* **2006**, *106*, 2711.
(30) Chaplin, D. A.; Johnson, N. B.; Paul, J. M.; Potter, G. A. *Tetrahedron Lett.* **1998**, *39*, 6777.

CG701211A